A case study of a remarkable tropopause folding over Eastern North America on March 14-15 2006.

Alain Robichaud
Atmospheric Science and Technlogy Branch
Environment Canada
2121 Trans-Canada Highway, 4th floor
Dorval, Qc, H9P 1J3
CANADA

(Internal report)

ABSTRACT

Stratosphere-to-Troposphere Transport (STT) is the most important natural factor contributing to the tropospheric ozone budget. STT also plays a key role in influencing the short term variability of water vapour of upper troposphere. Moreover, ozone tongues caused by tropopause folding can sometimes penetrate deeply into the troposphere producing irreversible transport and mixing of chemical species and tracers and affect surface conditions. This paper presents a recent case which occurred on March 14-15 2006 over Eastern North America where a deep and large stratospheric intrusion reached the surface. Observations, analyses outputs from different numerical models available at CMC (Canadian Meteorological Center) including a new coupled meteorological-chemical model are used to investigate the phenomena. These models are generally successful for representing the significant transport of stratospheric air mass to the lower troposphere. This is shown using various conservative quantities such as potential vorticity (PV) and different stratospheric constituents such as ozone and water vapour. In particular, results show the validity of using the ratio HNO_3/O_3 as a new tracer for detecting fresh stratospheric intrusions. However, a failure of models is the representation of the strong dehydration which occurred near the surface behind the cold front following the touchdown of stratospheric air. This phenomenon associated with the dry airstream circulation is well reported by the observation network. Large areas of very low water vapour mixing ratio ($< 10^{-3}$ kg/kg) at the surface were observed coincident with higher levels of surface ozone. Documentation of such extraordinary events is particularly important for model validation.

Introduction

Despite decades of observation, the connections between tropopause folding and near-surface conditions are still not very well understood. According to the literature, there are only a few documented studies of stratospheric air intrusions which have been confirmed to proceed all the way down to the ground**.** The most common synoptic feature responsible for this phenomenon are traveling cyclones which produce downward transport of upper atmospheric ozone (Sunwoo and Carmichael 1993). According to the mechanisms of cross-tropopause transport (Danielsen and Mohnen 1977), the highest convergence of ozone regularly occurs under the jet stream along the border of an upper trough. Only occasionally, the descent of air associated with a tropopause folding episode reaches the surface. Tropopause folds are the dominant and most efficient form of stratosphere-to-troposphere transport (STT) in the middle latitudes. Folds occurring within cut-off low systems has been widely documented (Price and Vaughan, 1993; WMO, 1986) and can have a significant impact on the tropospheric budget of constituents due to the downward transport of dry, ozone-rich stratospheric air. Stratosphere-troposphere exchanges are also important for a better knowledge of the interaction between chemical, dynamical and radiative features of the atmosphere on local to global scales (Holton et al., 1995). The deep exchanges are characterized by a 2-4 day life time and involve significant mixing of chemical species. However, most cross-tropopause exchanges are shallow and much of the air involved returns across the tropopause within 1 day (Stohl et al., 2003).

On the other hand, maximum values of surface ozone are usually associated with high anthropogenic emissions combined with higher temperatures and solar radiation which combine to enhance ozone photochemistry during summer. At remote sites in North America and Europe, however, at the surface, seasonal patterns with mean maxima in spring and mean minima in the cold season have been frequently observed (Singh et al. 1978). Some authors have attributed the surface spring maxima to stratospheric intrusions associated with tropopause folding events which activity also peaks in the spring (Altshuller 1986 ; Danielsen and Mohnen 1977). This hypothesis is recently questioned however by Stohl et al. (2003) who explained this maxima in terms of photochemistry rather than STT.

Episodes of stratospheric intrusions observed at many sites across the world have generally been related to the following meteorological conditions (Eisele et al., 1998; Keyser and Shapiro, 1986):

1. The axis of a jet stream is located near sites where surface higher levels of ozone were reported,
2. Rapid frontogenesis accompanied by a jet streak propagating into a trough,
3. Surface wind speed occurs predominantly from the northwesterly sector at those site,
4. A change to clear weather is observed, which is due to the subsidence process taking place,
5. The potential temperature is in the range 295-305 K.

In this paper, an example of stratospheric descent is shown as a case study. Objective analysis (OA) based on optimal interpolation (Ménard and Robichaud, 2005) has been constructed to analyze the surface distribution of ozone for a period of 5 years (2002 – 2006). Inspection of those analyses was the mechanism by which the strong tropopause folding event at study was detected by the lead author[1]. This OA is considered the best existing appropriate tool to analyze patterns of surface ozone in North America since it combines surface observations (from AIRNOW) and model output. It highlights important deficiencies of the Canadian air quality modeling system (CHRONOS) namely the absence of mechanism to take into account ozone intrusion of stratospheric origin. On the other hand, the meteorological GEM driver model could not reproduce extreme low values of water vapor near the surface which was reported behind the cold front by METAR[2] reports. Several diagnostics are assembled from various outputs of the Canadian NWP GEM model. For instance, a potential vorticity analysis constructed from output of the Canadian NWP GEM model (Global Environmental Multi-scale) is presented. Also, a study of METAR surface reports behind the cold front was performed and show astonishing low values of water vapor and relative humidity over a large area. All the information collected suggests a remarkable episode of tropopause folding and ozone transport from the stratosphere into the lower troposphere on May 14-15 2006 over Eastern North America. Finally, we show that a new tracer (ratio HNO_3/O_3) originally proposed by Dibb et al (2006) in the context of aircraft measurements, when applied to numerical models gives a very interesting signature

---

[1] A suspicious surface ozone rise immediately behind a leading cold front was then noted on March 14th 2006 over Southern US on the OA map.

[2] METAR are hourly surface meteorological observation at aerodromes.

of fresh stratospheric intrusions. In section 4, this ratio is obtained from model outputs of a new coupled dynamics-chemistry model, the GEM-MSC-BIRA model.

2. Synoptic situation over Eastern North America on the 14 March 2006.

According to the surface CMC analysis, a deepening low pressure system crossed the upper Great Lakes between 13th -14th of March 2006 (figure 1). At 18Z, on the 14th, the main surface low was centered in Northwestern Quebec with a pressure center at about 980 hPa accompanied by a secondary development off the New England coast. A vigorous cold front (leading front) extended from the developing low off the New England coast to the south and then curved back to southwest into the Gulf of Mexico. During the course of the day, a satellite animation loop reveals that the southern extent of the front was crossing the southern states of US at a moderate speed (animation not shown). Note that a secondary cold front immediately behind was found much less active as compared to the leading one. However, both fronts were associated with a well organized jet stream core aloft. Figure 2 presents a map of the wind speed evaluated from the GEM global model near 250 hPa valid at 18Z. We can see three different jet streams (J1,J2 and J3 indicated by dash circles on figure 2) which all converge over the region of interest. Figure 3 shows a map of the geopotential height at 250 hPa. A pronounced trough dominates the Eastern parts of North America. The estimate position of the tropopause folding is depicted by the dashed circles (see section 4b for further explanation). At 500 hPa (figure 4), a confluence area (indicated by a tighter horizontal gradient of the local geopotential field) is obvious over the Eastern US. At all altitudes, a closed circulation has started to form just North of the Great Lakes (cut-off low). In summary, an intense and organized upper wind circulation is present over Eastern United States. GOES-12 infrared satellite picture clearly depicts the position of a sharp katabatic cold front at 2215Z over Eastern North America associated with the storm (Figure 5). At 2215Z, the front was lying from Halifax to a position roughly parallel to the US Eastern seabord and curved back to Northern Florida and then to the Gulf of Mexico to finally dissipate into North East Mexico. A well defined dry slot was also visible along the coast from New England down to Virginia and a typical "comma shape" cloud structure was clearly visible over Eastern North America. A great deal of subsidence accompanied the cold front. This is confirmed by the water vapor channel picture taken few hours earlier (figure 6). According to Appenzeller et al. (1986), the dark band in the water vapour channel should indicate the intrusion of stratospheric air in the troposphere. But, in this case at study, it seems that the darkest area corresponds to a location where the dry airstream (DA)[3] penetrates the boundary layer and where the lowest surface relative humidity is reported (see section 4 and 5). Independent surface METAR reports almost simultaneously indicate relative humidity readings near or below 10 % on many stations over the Southern Eastern US with one station reporting a dew point temperature as low as -48° C corresponding to relative humidity of less than 1 %[4]. Water vapour content in the lower stratosphere is typically one or two order of magnitude less, in comparison with the troposphere. Reports of relative humidity below 10-15% (roughly corresponding to mixing ratio less than 1 g/kg at mid latitudes) at various places for several hours suggest a

---

[3] For explanation about the concept of dry air stream, see Carlson, 1988.

[4] Note that the precision of the hygrometer is about 1.5 deg for the range of dew point from -10 to -40C so that the low values reported are not believed to be an artifact of the measurement system.

stratospheric origin. Fig. 10 shows the time evolution of the relative humidity for several stations (the locations of different stations are indicated in figure 9).

3. Model outputs, data and analysis.

Model and analysis outputs used in this study are briefly described below:

- CHRONOS: The Canadian Hemispheric and Regional Ozone and NO_x System has been designed for the prediction of atmospheric oxidants on both regional and hemispheric scales. The original version of the system is described in Pudykiewicz et al. (1997). Up to now, the model has been used for real-time air quality forecasting in Canada. An Objective analysis (OA) (figure 7, right top panel) combining CHRONOS model output (top, left panel) with AIRNOW-EPA surface ozone data (bottom right panel) is available on a near real time basis at the Canadian Meteorological Center (CMC). Analysis increments are correction to the model (bottom left panel). Details about this OA are given in Ménard and Robichaud (2005).

- GEM Operational Model (Global, Environmental, Multi-scale model, Coté et al, 1998a,b) is a global variable resolution model using semi-implicit and semi-Lagrangian numerical techniques. It is part of 4D-Var assimilation system and currently used for meteorological operations at the CMC. It runs at a resolution of 0.9^o on 28 vertical levels with a lid at 10 hPa. The GEM-Regional version of the model has a resolution of 15 km, 58 levels and uses a 3DVAR-FGAT assimilation scheme (three-dimensional variational analysis with first guess at appropriate time for dynamic assimilation) and an ISBA land scheme (Interface Soil-Biosphere-Atmosphere).

- GEM-MSC-BIRA: This experimental version of GEM is a coupled meteorological-chemistry model for the study of stratospheric phenomena. The model is coupled with an on-line photochemical module from BIRA[5] which includes 57 advected species and about 200 photochemical reactions. The initial condition is obtained from ECMWF (for dynamic fields) and BIRA (for chemistry fields) hence providing complete analyses from the surface up to 0.1 hPa. An assimilation system based on 3D-VAR FGAT was run for two weeks before the event to insure consistency and avoid spin-up problems. No assimilation of ozone was performed in this case study.

---

[5] BIRA: Belgium Institute of Research in Aeronomy located in Brussels.

4. Observational evidence of a folding

a. Surface ozone field

The tropopause folding was first detected indirectly through routine monitoring of surface OA as already mentioned. The frontal position as seen from satellite picture (figure 5) and the leading edge of the 40 ppbv surface contour of ozone in figure 7 (top right panel) almost perfectly coincide. Animation of satellite and objective analysis map for that day showed simultaneous motion towards the East for both features. The increase of ozone behind the cold front is therefore mostly associated with an ozone-rich air mass behind the leading edge of the front which is rather abnormal. Usually, the ozone concentrations behind a front decrease due to advection of clean air masses or enhanced cloudiness which prevents the photochemical production of ozone by nitrogen oxides, volatile organic compounds and heterogeneous chemistry. In some rare cases the concentrations increase due to downward mixing of ozone enriched air intruded from the stratosphere into the troposphere by tropopause foldings. On the other hand, higher surface ozone levels and smog usually occur ahead of cold front in warm sectors or associated with slowly migrating anticyclones (Altshuller, 1978; Heidorn and Yap, 1986) providing plenty of solar radiation, higher temperatures, light winds and vertical mixing. The abnormal pattern observed on March 14th 2006 could only be explained in terms of a powerful dry air stream reaching the surface and producing the unexpected ozone rise. This effect could not be simulated by CHRONOS[6] but has been captured by the OA. The analysis increments (figure 7, bottom left panel) represent a correction to the model and show a large area of positive increment related to the stratospheric contribution to surface ozone over Gulf Coast states and South Eastern states of US. Indeed, the coincidence between the ozone rise and dehydration region near the surface (figures 11 and 16) is attributed to the stratospheric origin of the air parcels.

b. Measurements of satellite ozone total column

A close relationship has been shown to exist between total ozone column measurement and cyclonic system features (Olsen et al., 2000, Price and Vaughan, 1993). Since total ozone is the integrated ozone profile through the depth of the atmosphere and since this quantity depends on air density, then ozone-rich stratospheric air at tropospheric heights gives a significant contribution to the total ozone column. An increase of about 100 DU (Dobson Unit) on total ozone column has been attributed to tropopause folding by Olsen. Figure 8 shows global coverage satellite measurement of total column ozone for March 14th 2006 made by the instrument OMI (Ozone Monitoring Instrument) mounted on AURA satellite. A " hook" pattern of higher total column ozone over North America centered around 45 deg. N, 90 deg. W roughly corresponds to the western and southern flank of the cut-off low (see dash circles of figure 3) roughly in agreement with the analysis of Olsen et al. (2000). The position of the "hook" (averaged through the day of March 14) would indicate the approximate location of the tropopause folding. This ozone was then transported further down and further south by the DA explaining higher values of surface

---

[6] Chronos has a model lid at 8 km and has no provision to take into account stratospheric ozone.

ozone than expected (figure 7) and very low relative humidity over a large region in Southeastern US (figures 11 and 16).

c. Study of water vapor and relative humidity

Water vapor can also be used as a tracer for detecting the transport of air from the Upper Troposphere Lower Stratosphere (UTLS) region to the surface within the DA circulation. Figure 6 shows the GOES water vapor channel for March 14th 2006 at 1815Z. A very dry area is evident just behind the leading front position (see figure 1 and 5 for the front location) up to about 500 km behind the position of the leading cold front. This band is believed to be the position where the DA penetrated the planetary boundary layer (PBL). An another dark area although weaker (wrapped around the cut-off low) is associated with the folding itself (roughly corresponding to the dash circles in figure 3). The dark area associated with the dry air stream reaching the surface is presumed to be where the water vapor in the column is the lowest at the time of the picture and where one is most likely to find the lowest values of surface water vapor and relative humidity. Figure 11 shows GEM model output for specific humidity near 850 hPa at 18Z. Across the cold front, we observe a drop of two order of magnitude for water vapor mixing ratio. Values range from about 12-15 kg/kg ahead of the cold front in Gulf of Mexico down to about 0.1 kg/kg or less behind. Model results are realistic outside the PBL but are too large near the surface compared with many METAR surface measurements which report relative humidity (RH) near or below 10%. In particular, an exceptionally low value of 0.4% at the station KJNX in North Carolina (temperature = 21°C, dew-point temperature = -48°C at 20Z) was reported corresponding to a mass mixing ratio of 5.8E-5 kg/kg for water vapor mixing ratio which is typical of tropopause values. Figure 10 show the time evolution of relative humidity on March 14-15 2006 for selected stations (location shown in figure 9). It indicates that stratospheric air deeply influenced the surface water vapor for almost 12 hours at many stations which is considered to be a rare event.

5. Model diagnostics

a. Analysis of potential temperature and potential vorticity

Potential temperature is the temperature an air parcel would have if expanded or compressed adiabatically (i.e., without any heat being added or taken away) from its existing pressure to a reference pressure, usually taken to be 1000hPa or 1000mb. It is usually denoted θ and may be calculated from the formula

$$\theta = T \, (P_o/P)^{(R/c_p)}$$

where P and T are the parcel's pressure and temperature, P_o is the reference pressure, R is the gas constant for air, and c_p is the specific heat capacity at constant pressure for air. Figure 12 presents a meridional cross section of potential temperature at 18Z for March 14th 2006 from GEM-Regional model. The cross section is taken along the arrow shown on figure 11 which is located almost orthogonally to the cold front (roughly from South to

North from Gulf of Mexico to Michigan along longitude 85W). Descending air approximately follows isentropes.

On the other hand, high values of Potential Vorticity (PV) occur in the stratosphere while lower values are found in the troposphere. The tropopause is dynamically defined, namely through a threshold value of potential vorticity (PV). This threshold lies between PV values range from 1.5 PVU and 2.5 PVU (Meloen et al., 2001), where

$$1PVU = 10^{-6} m^2 K \ kg^{-1} s^{-1}$$

Note that the conventional definition for the tropopause is 1.6 PVU (World Meteorological Organization 1986, chapter 5). Potential vorticity is a function of the atmospheric static stability, and the stratosphere is therefore a reservoir of high values of PV. Anomalously large values of PV found in the troposphere generally indicate the presence of air originating in the stratosphere. Potential vorticity in adiabatic, frictionless flow is defined as a product of absolute vorticity and static stability. The formal definition of Ertel potential vorticity, based on potential temperature θ is

$$Q = -g(\zeta_\theta + f) \ d\theta/dp.$$

This equation is valid for large-scale, hydrostatic flow. The potential vorticity is conserved following 3D, adiabatic, frictionless flow. Therefore, along an isentrope surface, Q is conserved. This means that as air parcels enter the troposphere from the stratosphere their potential vorticity must increase since the static stability decreases. Figure 13 shows a meridional cross section of Ertel`s potential vorticity (PV) computed using output fields from the GEM regional model (resolution of 15 km)[7] clearly suggesting at least two stratospheric intrusions associated with the tropopause folding event. In fact, a third intrusion seems to be also present (north of the domain of figure 13) but was not considered in the context of this paper. The first intrusion is associated with a jet stream located at about level .22 sigma in the middle of the domain (which corresponds to J1 of figure 2). The downward and equatorward descent of slightly higher PV is noticeable although a lot of mixing is present. The second intrusion is more pronounced and occurs at a lower altitude (about 0.46 sigma level and is likely to be related to J2 in figure 2). The white area corresponds to values greater or equal to 2 PVU indicating air of stratospheric origin. PV is a surrogate for ozone in estimating its amount transported into the troposphere. Although model does not show that stratospheric air reaches the surface, it clearly shows the downward extent of an anomalously high PV tongue extending equartorward and descending along isentropes. Boundary layer mechanisms such as eddy diffusion likely prevent the descending tongue to reach the surface. Comparing figures 12 and 13 suggest that the descent took place roughly along the 295-300 deg. K isentrope. Eisele et al (1999) reported stratospheric intrusions associated along potential temperature in the range 295-305K which compares well with the results obtained from this case study.

---

[7] The highest resolution model at CMC (GEM regional) is used to calculate potential vorticity since PV is rather sensitive to vertical resolution.

b. Analysis of stratospheric tracers

Figure 14A shows a cross-section of ozone mixing ratio from the stratospheric GEM-MSC-BIRA model with a lid at 0.1 hPa (the cross section is also taken along the arrow of figure 11). Results indicate similarly a downward extent for the ozone tongue roughly which coincide with the region of large PV shown in figure 13. Considerable model diffusion occurs on its way through the troposphere so that the mixing ratio diminishes during the descent. Nevertheless, the dimension of the descending ozone tongue remains quite large and well resolve by the global model. Figure 14b shows that other stratospheric long lived constituents such as HNO_3 can be used for diagnosis of STT events. An excellent tracer for detecting stratospheric air intrusion is the ratio HNO_3/O_3 (as suggested by Dibb et al., 2006 based on aircraft measurements) who identified that values of that ratio between 2-4 E-3 reveals the signature of air parcels originating from the tropopause. Results from GEM-MSC-BIRA (figure 14c) shows ratio values within the critical range which provides evidence of a deep and wide fresh stratospheric intrusion. A closer look at model simulation suggests than a range of values for the ratio HNO_3/O_3 from 1.7 to 3.0 E-3 describes more accurately the stratospheric intrusion at study. It is argued that this new tracer is more precise and give a sharper edge than more conventional diagnostics such as PV and ozone because it is less affected by diffusive processes since the influence cancels out when a ratio of two tracers is taken. A high ratio (HNO_3/O_3) at tropospheric location more clearly indicate the position of a stratospheric intrusion compared with PV or ozone. According to figure 14c, the horizontal dimension of the tongue is approximately estimated to about 500-700 km wide between the levels 500-250 hPa. Finally, this new tracer (HNO_3/O_3) is thought to be superior to the commonly used Be-7 (Beryllium-7) tracer in the detection of intrusions. Although correlations between Be-7 and ozone identify the presence of stratospheric air, such data are not sufficient to quantify the stratospheric contributions, as ozone is also produced at ground level. According to Dutkiewicz and Husain (1985), only 23-27% of the Be-7 in surface air at northern mid-latitudes is of stratospheric origin. Moreover, the half-life of Be-7 being about 50 days makes it difficult to precisely identify the age of the stratospheric intrusion. The rise of Be-7 at a particular level could have been the result of a STT which had occurred anytime and anywhere over the past 50 days or so. Finally, Be-7 and similar radionucleides cannot be considered as ideal stratospheric tracer because they are attached to aerosols so that their tropospheric lifetime is dictated by wet scavenging processes. The ratio of Be-7 over Be-10 is presented as an alternative by Zanis et al (2003). However, it suffers from the fact that Be-10 measurements are difficult to obtain since it requires the technique of accelerator mass spectrometry which is an expansive method of continuous monitoring.

c. Model analysis of surface water vapour

Comparison with observation and different models have been done for water vapor within the PBL. Figure 15a, b and c show vertical profiles of water vapour mixing ratio from three different models used at CMC. The profiles are all taken in Northern Carolina near the station KJNX (see figure 9 for the exact location). All model show very low water vapour mixing ratio (less than 1 E-3 kg/kg) from the stratosphere down to about 900 hPa[8] but are too humid within the PBL and

---

[8] That is about 0.9 in hybrid or sigma coordinate system

at the surface. The mean surface observations average out to about 4.0E-4 kg/kg at 00Z[9]. For convenience, on figures 15, this value is reported as a red cross (surface level). We estimate that the model surface values are too humid by a factor of about 3.5 for GEM-Regional (surface model value of 1.42E-3 kg/kg) and almost one order of magnitude for GEM global models (2.90E-3 for GEM-MSC-BIRA and 4.19E-3 for GEM-Global operational). Figure 16 shows a more comprehensive comparison of the GEM-Regional model (the model with the highest horizontal resolution) with observations of surface dew point depression (obtained from METAR observations) valid at 21Z, March 14th 2006. The significant mismatch between model (background colors) and observations (colored squares) can be due to several PBL processes including the model representation of soil moisture fluxes and subgrid mixing processes. Note that comparison with upper air radiosondes was not undertaken since the detection of very dry layers are difficult due to the tendency for meteorological agencies to systematically clip the observed values of the dew point depression ($T-T_d$) to a maximum of 30 degrees destroying the signal of an air mass having stratospheric origin.

6. Summary and conclusion

Measurements and model analyses showed evidences of a remarkable tropopause folding which occurred over Eastern North America on 14-15 March 2006. This event was particularly strong and has produced a deep intrusion of stratospheric air which has reached the surface. The associated exchanges processes had a significant impact on the surface budget of the main atmospheric constituents such as water vapour and ozone. During the period, METAR surface observations have reported values of specific humidity below 10^{-3} kg/kg over a wide area which is associated with the transport of dry air from the tropopause region. Right behind the leading edge of the cold front, a surface analysis map of ozone (OA) detected a sudden increase of ozone. Moreover, a signature is clearly present in the satellite total ozone column corresponding to an increase of PV. Those observations all point to the stratospheric origin of the tropospheric air parcels.

The system at study has been analyzed using different models to identify the processes involved. Results have demonstrated that the transport of quasi-conservative quantities such as potential temperature and potential vorticity gives a realistic signature of the stratospheric intrusion within the troposphere. A stratospheric coupled model with on-line chemistry has been used to follow the evolution of stratospheric constituents such as ozone. It clearly indicated the increase of the downward transport of ozone-rich stratospheric air which caused column ozone increase seen in the measurements. Other tracers such as the ratio HNO_3/O_3 was also used to identify more accurately the descent of air at tropospheric levels. Results showed the limitation of the current operational modelling and observation system which are not designed to resolve such events. It also suggest the necessity to incorporate stratospheric processes into existing NWP and AQ models. The study also indicates that models fail to reproduce the strong dehydration which sometimes occurred behind the cold front at the surface. Studies of such events are particularly useful for model validation purpose.

---

[9] This value is obtained by simply taking the mean value of mixing ratio at KJNX, KASJ and KHRJ which are the three closest stations around the location of vertical profiles of figure 15.

7. References

Altshuller, A.P., 1978. Association of oxidant episodes with warm stagnating anticyclones. J Air Pollut Control Assoc 28: 152-155.

Altshuler, A. P., 1986: The role of nitrogen oxides in non-urban ozone formation in the planetary boundary layer over N. America, W. Europe and adjacent areas of ocean. *Atmos. Environ,* **20,** 245–268.

Appenzeller, C., Davies, H. C., and Norton, W. A.: Fragmentation of stratospheric intrusions, J. Geophys. Res., 101, 1435–1456, 1996.

Carlson T., 1998. Mid-Latitude Weather Systems. American Meteorological Society, Boston, 1998.

Coté, J., S. Gravel, A. Méthot, A. Patoine, M. Roch, and A. Staniforth. The Operational CMC-MRB Global Environmental Multi-scale (GEM) Model. Part I: Design onsiderations and formulation. *Monthly Weather Review*, 126, 1373-1395, 1998a.

Coté, J., J.-G Desmarais, S. Gravel, A. Méthot, A. Patoine, M. Roch, and A. Staniforth. The Operational CMC-MRB Global Environmental Multi-scale (GEM) Model. Part II: Results. *Monthly Weather Review*, 126, 1397-1418, 1998b.

Danielsen, E. F., and V. A. Mohnen, 1977: Project report: Ozone transport, in situ, measurements, and meteorological analyses of tropopause folding. *J. Geophys. Res.,* **82,** 5867–5877.

Dibb J.E, Scheuer E., Talbot R. , 2006. Stratospheric influence on the composition of the mid and upper troposphere over North America sampled by the NASA DC-8 during INTEX A. Submitted to *Journal of Geophysical Research*, special section on INTEX A.

Dutkiewicz V.A., Husain L, 1985. Stratospheric and tropospheric components of Be-7 in surface air. J. Geophys. Res., 90, 5783-5788, 1985.

Eisele, H., E. Scheel, R. Sladkovic, and T. Trickl, 1998. High-Resolution Lidar Measurements of Stratosphere–Troposphere Exchange. Journal of the Atmospheric Sciences, vol. 56, No. 2, pp. 319-330.

Heidorn K., Yap D., 1986. A synoptic climatology for surface ozone concentrations in Southern Ontario: 1976-1981. Atnospheric Environment, 20, pp. 695-703.

Holton, J. R., Haynes, P. H., McIntyre, M. E., Douglass, A. R., Hood, R. B., and Pfister, L.: Stratosphere-troposphere exchange, Rev. Geophys., 33, 403–439, 1995.

Keyser D., Shapiro M.A., 1986. A review of the structure and dynamics of upper level frontal zones. Mon. Weather Rev., 114, pp 452-499.

Ménard R., Robichaud A., 2005. The Chemistry-Forecast System at the Meteorological Service of Canada. Proceedings of ECMWF Seminar on Global earth-system monitoring, 5-9 September 2005. Available at ECWMF web site (annual seminars).

Meloen, J., P.C. Siegmund and M. Sigmond, 2001. A Langrangian computation of stratospheree-troposphere exchange in a tropopause folding event in the subtropical Southern Hermisphere. Tellus, 53(3), 367-378.

Olsen, M. A., Gallus, W. A., Stanford, J. L., and Brown, J. M.: Fine scale comparison of TOMS total ozone data with model analysis on an intense mid-western cyclone, J. Geophys. Res., 105, 20487–20495, 2000.

Price J.D., Vaughan G., 1993. The potential for stratosphere-troposphere exchange in cut-off low systems. Quarterly Journal of Royal Met. Society, 119, pp 343-365, 1993.

Pudykiewicz J., A. Kallaur, and P.K. Smolarkiewicz, 1997. "Semi-Lagrangian modeling of tropospheric ozone. Tellus, 49B, 231-248.

Singh, H., F. L. Ludwig, and W. B. Johnson, 1978: Tropospheric ozone: Concentrations and variabilities in clean remote atmosphere. *Atmos. Environ.,* **12,** 2185–2196.

Stohl, A., Wernly, H., James, P., Bourqui, M., Forster, C., Liniger, M. A., Seibert, P., and Sprenger, M.: A new perspective of stratosphere-troposphere exchanges, Bull. Amer. Meteor. Soc., 84, 1565–1573, 2003.

Sunwoo, Y., and G. R. Carmichael, 1993: Tropospheric ozone production, transport, and distribution in the Western Pacific Rim. *Proc. Int. Conf. on Regional Environment and Climate Changes in Eastern Asia,* Taipei, Republic of China, 113–117.

World Meteorological Organization, 1986: Atmospheric ozone 1985: Global ozone research and monitoring report. WMO Rep. 16, 392 pp.

Zanis P., T.Trickl, A. Stohl, H. Wernli, O. Cooper, C. Zerefos, H. Gaeggeler, C. Schnabel, L. Tobler, P.W. Kubik, A. Priller, H.E.Scheel, H.J.Kanter, P.Cristofanelli, C. Forster, P. James, E. Gerasopoulos, A. Delcloo, A. Papayannis and H. Claude, 2003. Forecast, observation and modelling of a deep stratospheric intrusion event over Europe. Atmos. Chem and Physics Discussions. EGU 2003, Vol 3. pp 1109-1138.
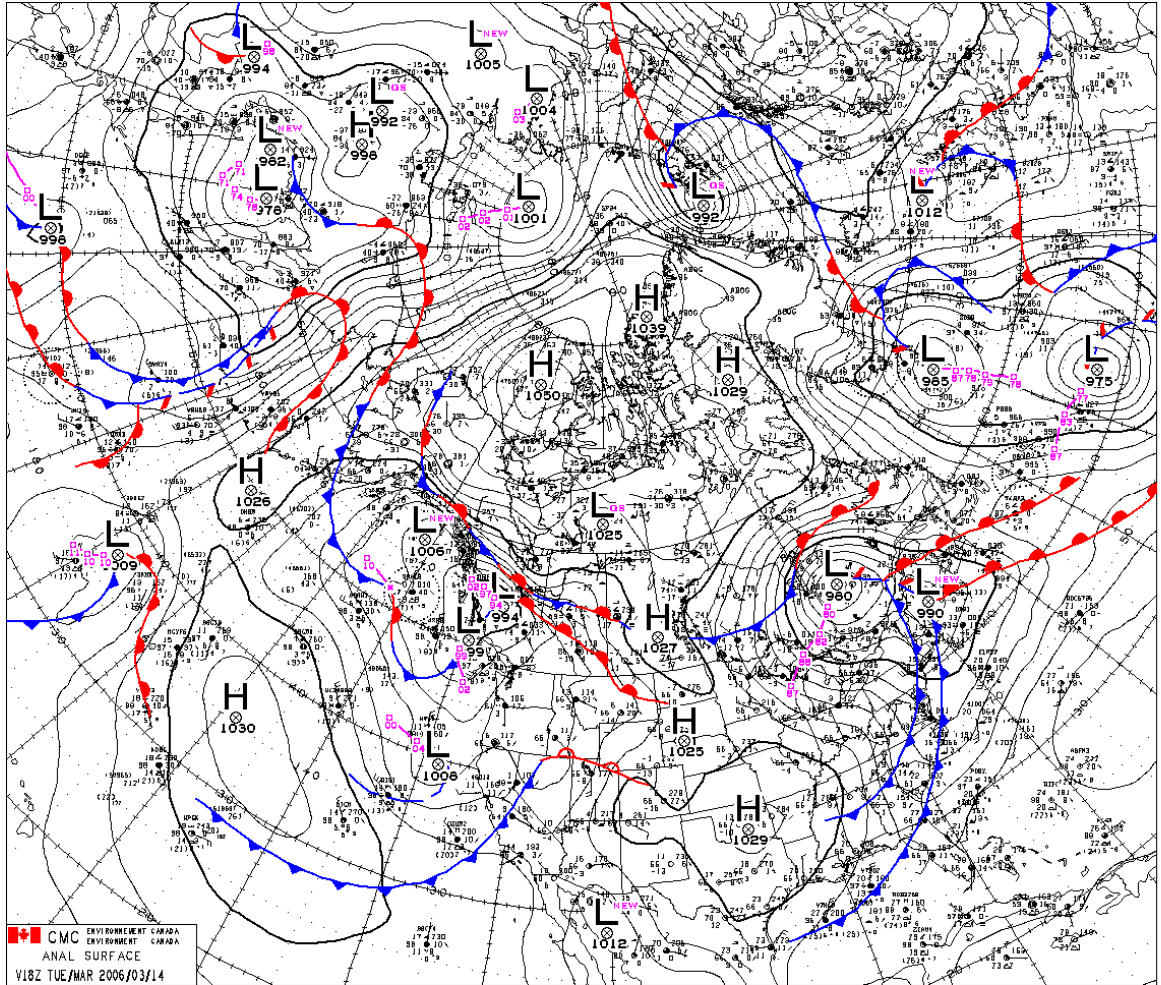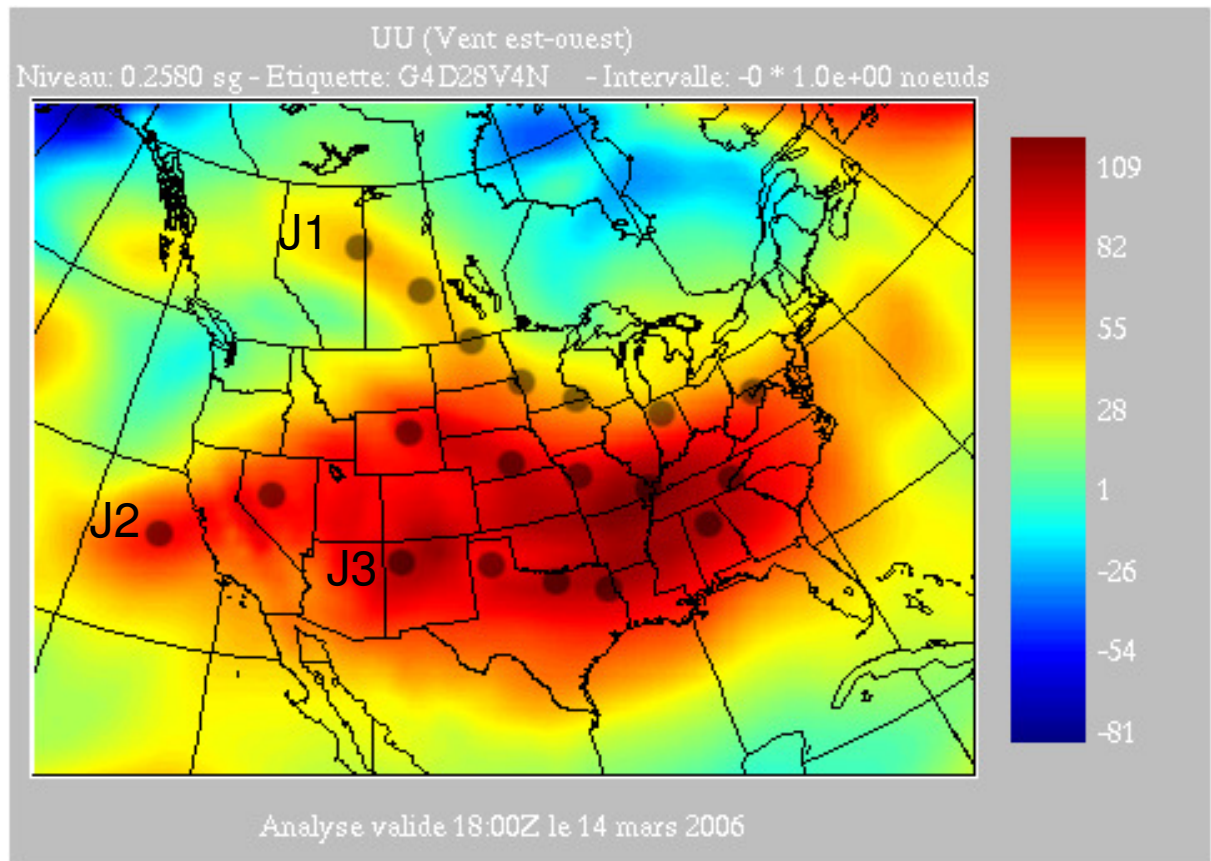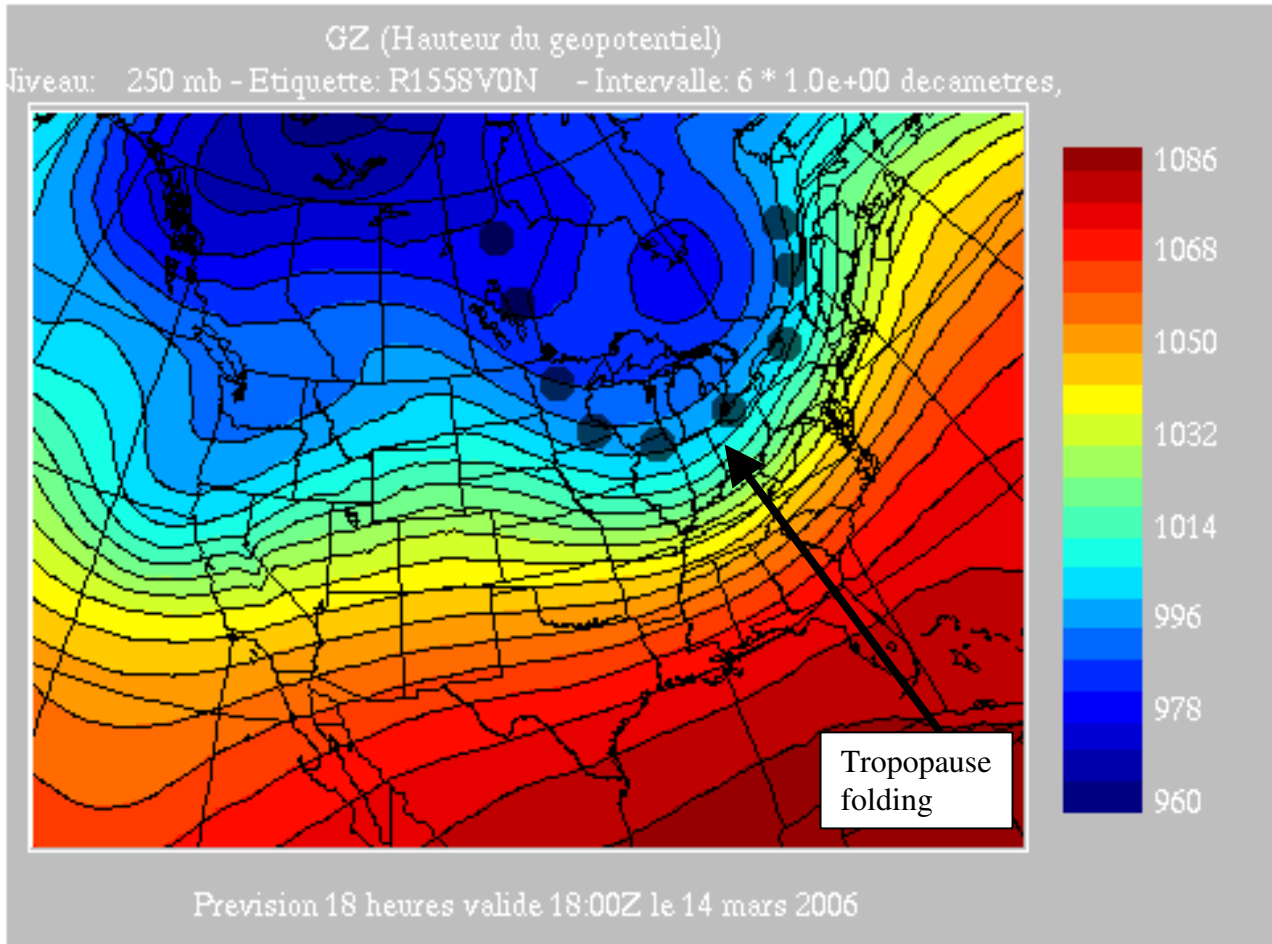
FIGURE 1

FIGURE 2

FIGURE 3
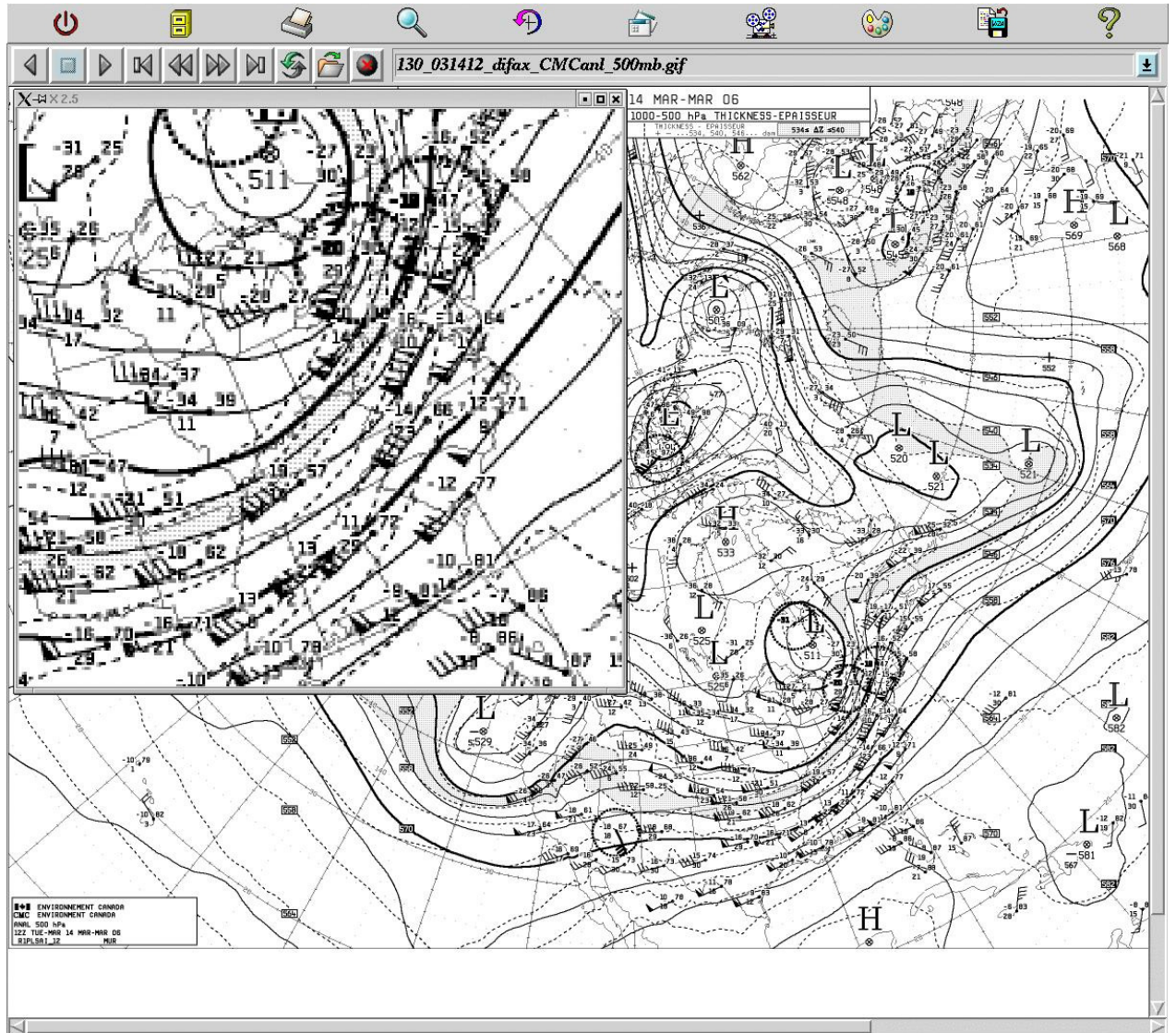
FIGURE 4
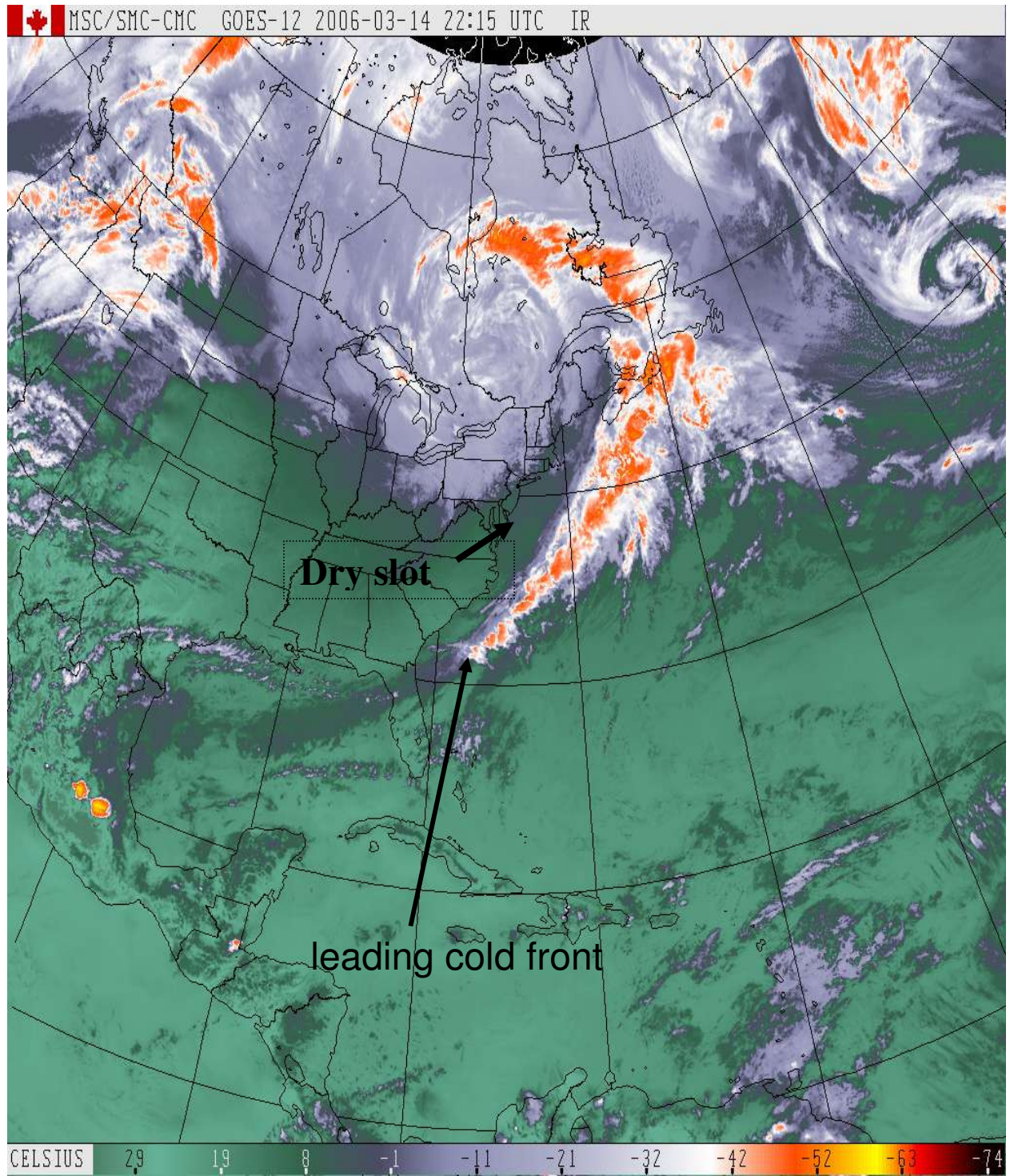
FIGURE 5
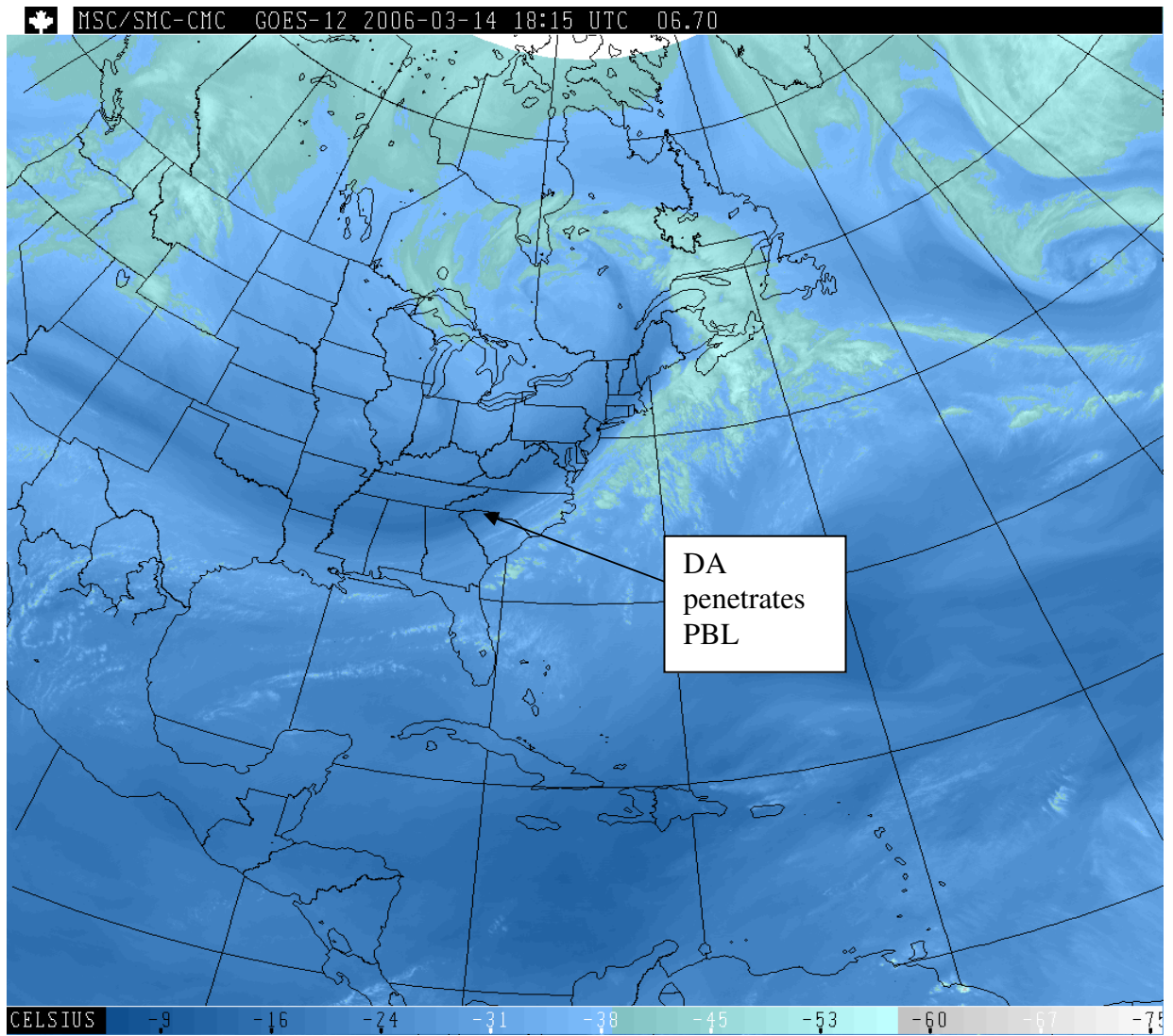
FIGURE 6

FIGURE 7

OMI Total Ozone Mar 14, 2006

Tropopause folding

NIVR−FMI−NASA−KNMI

OMI

Dobson Units
Dark Gray < 100 and > 500 DU

GSFC

NASA
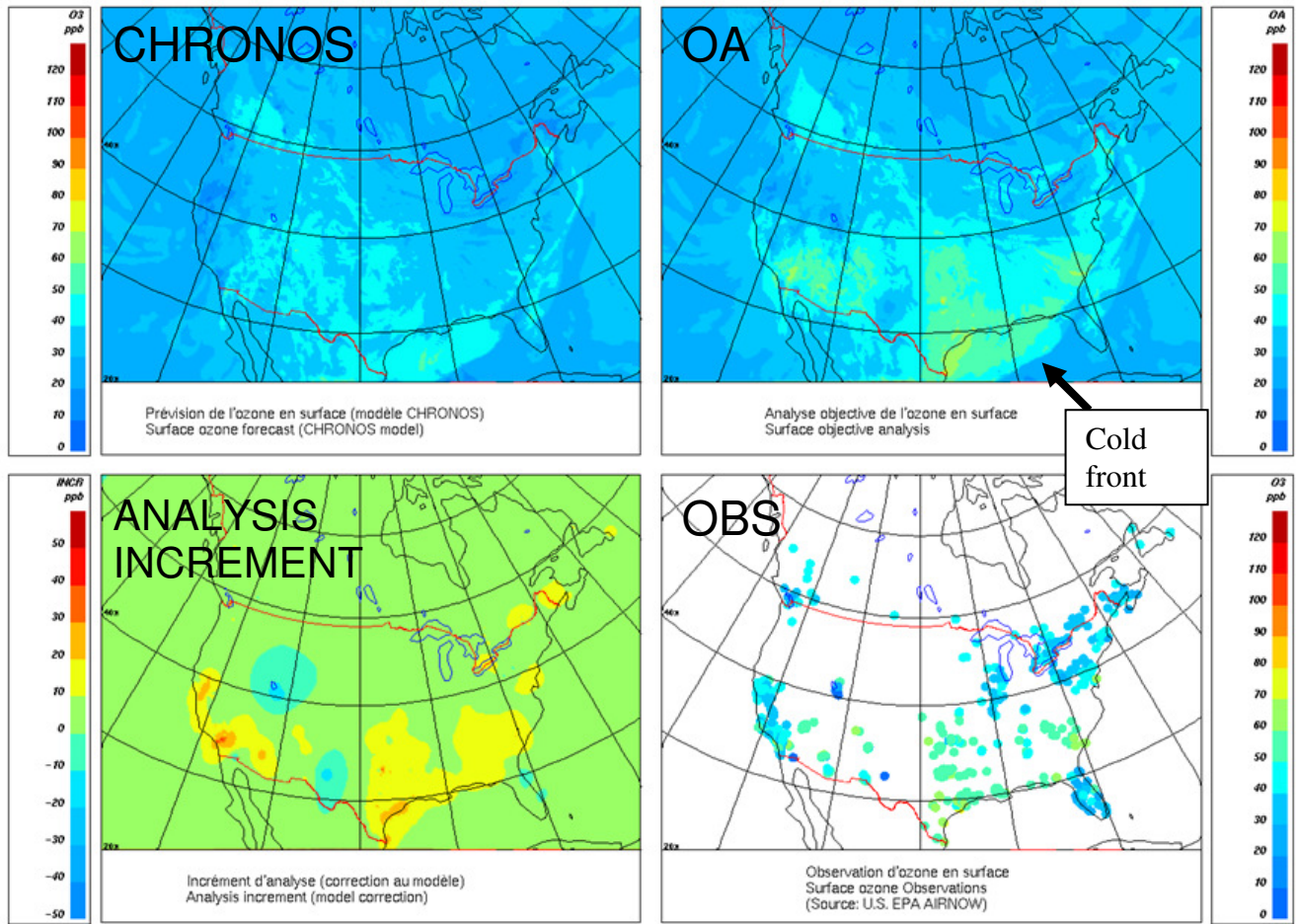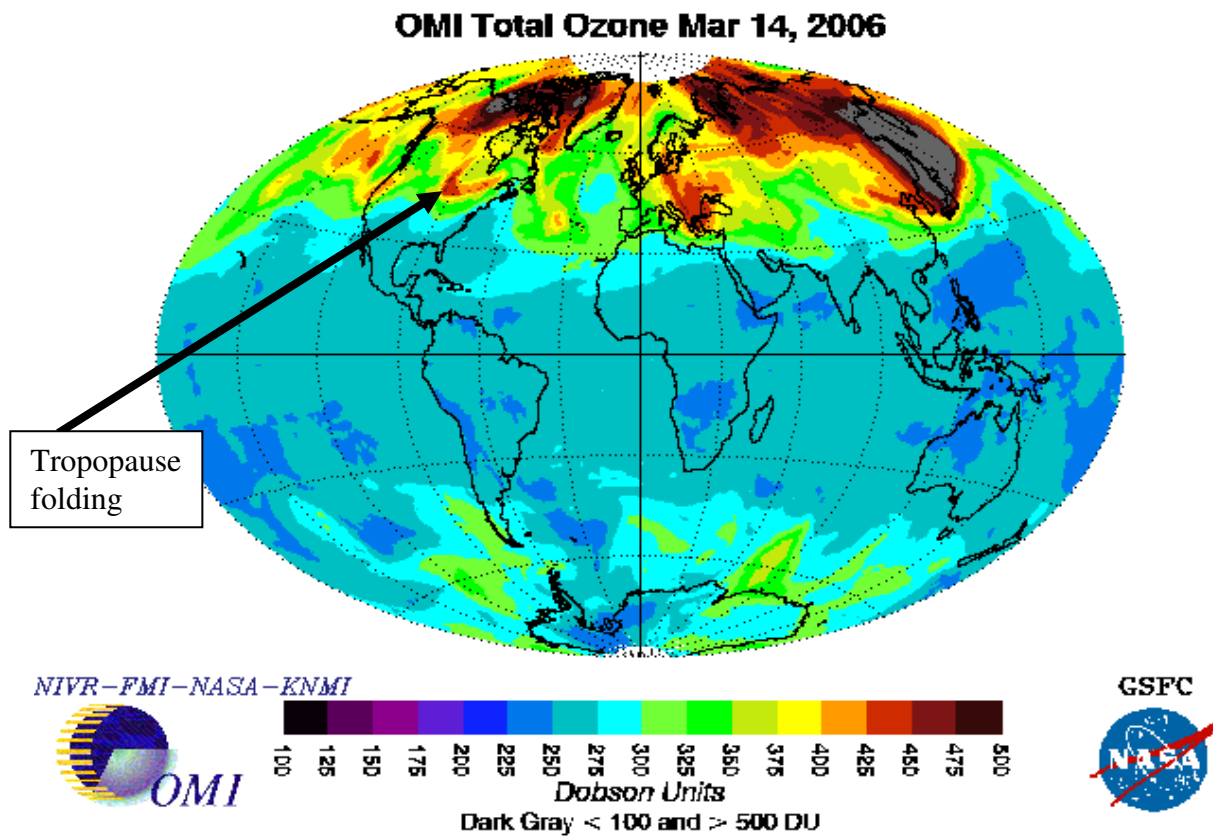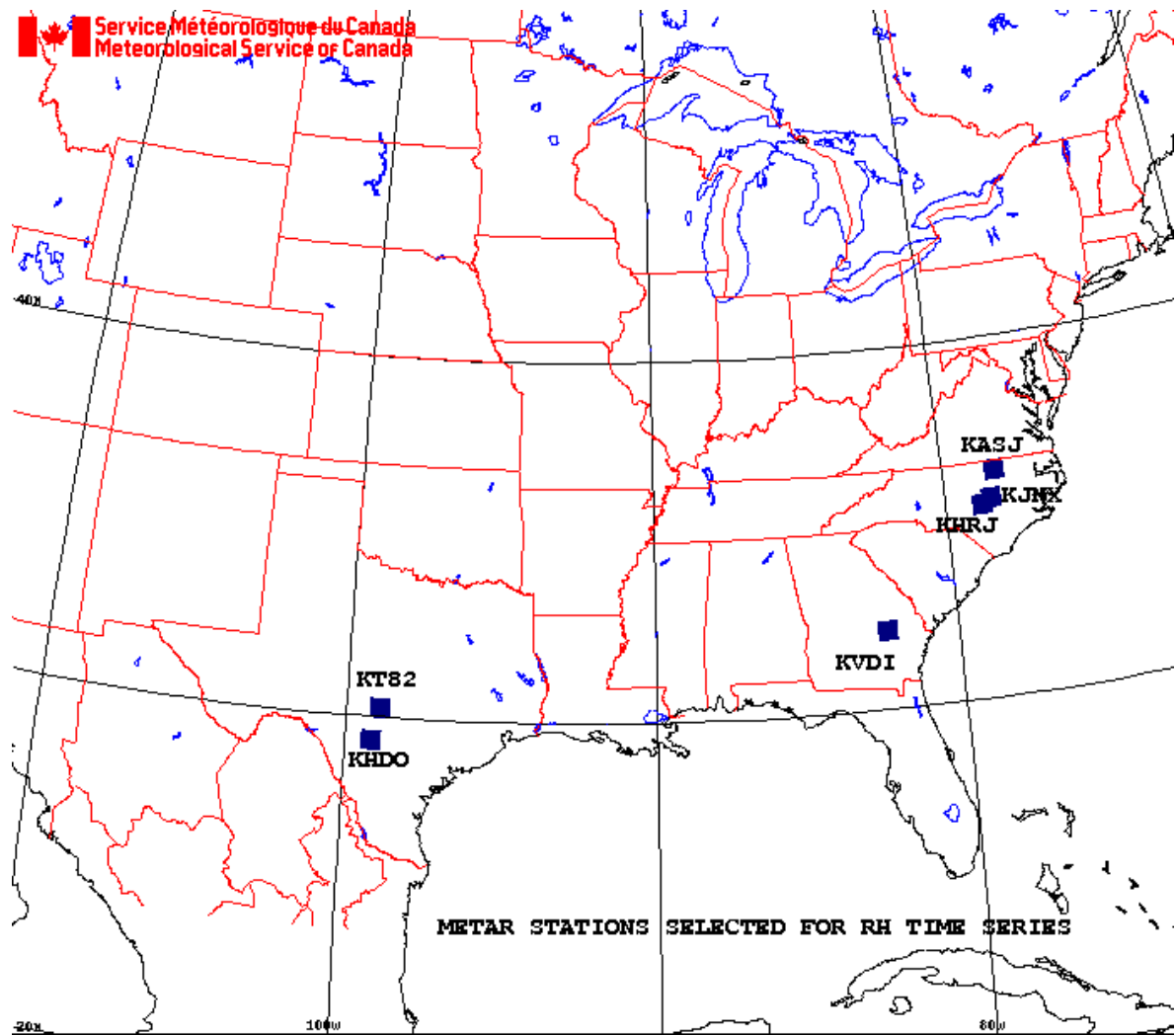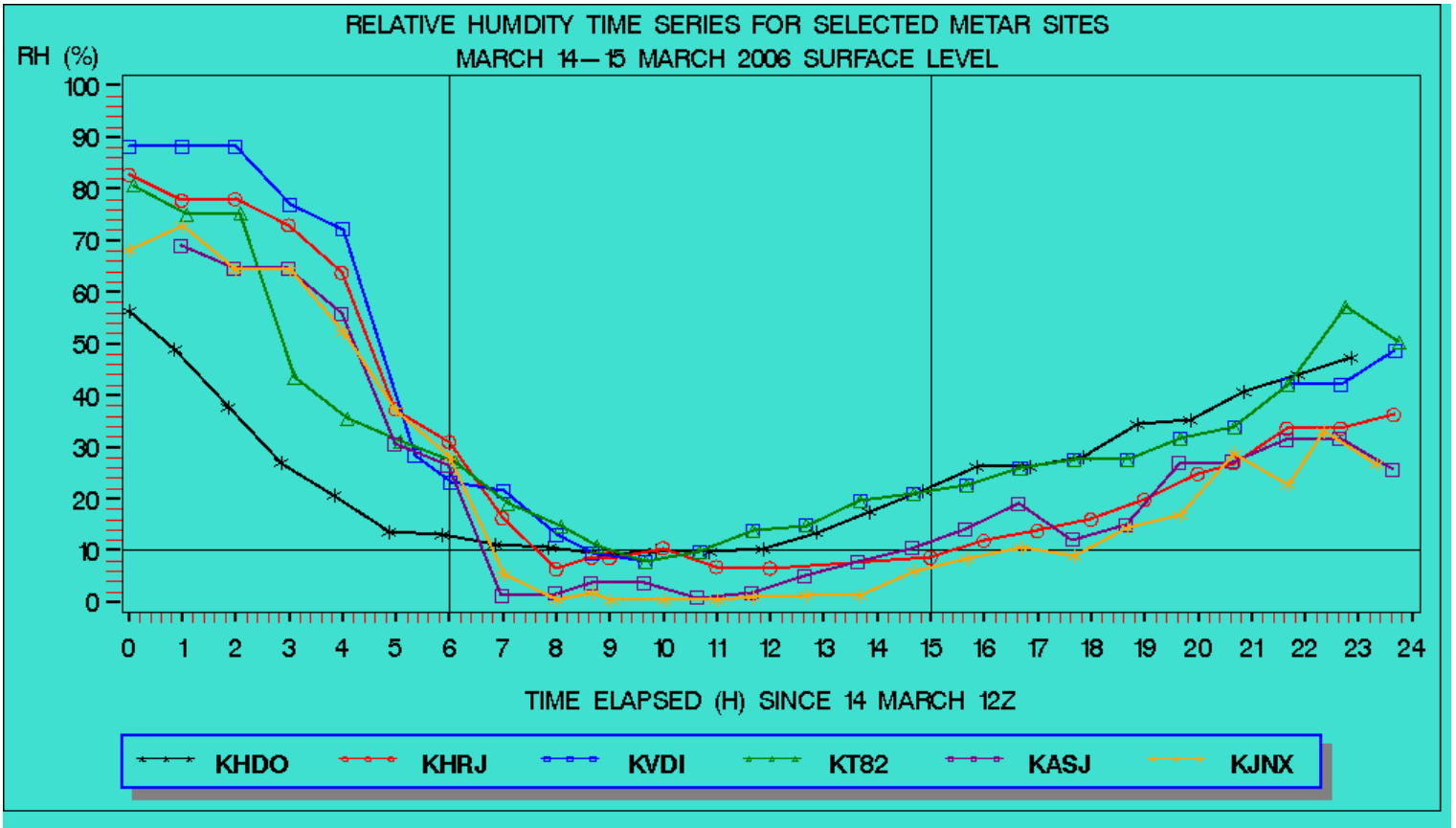
FIGURE 8

FIGURE 9

FIGURE 10
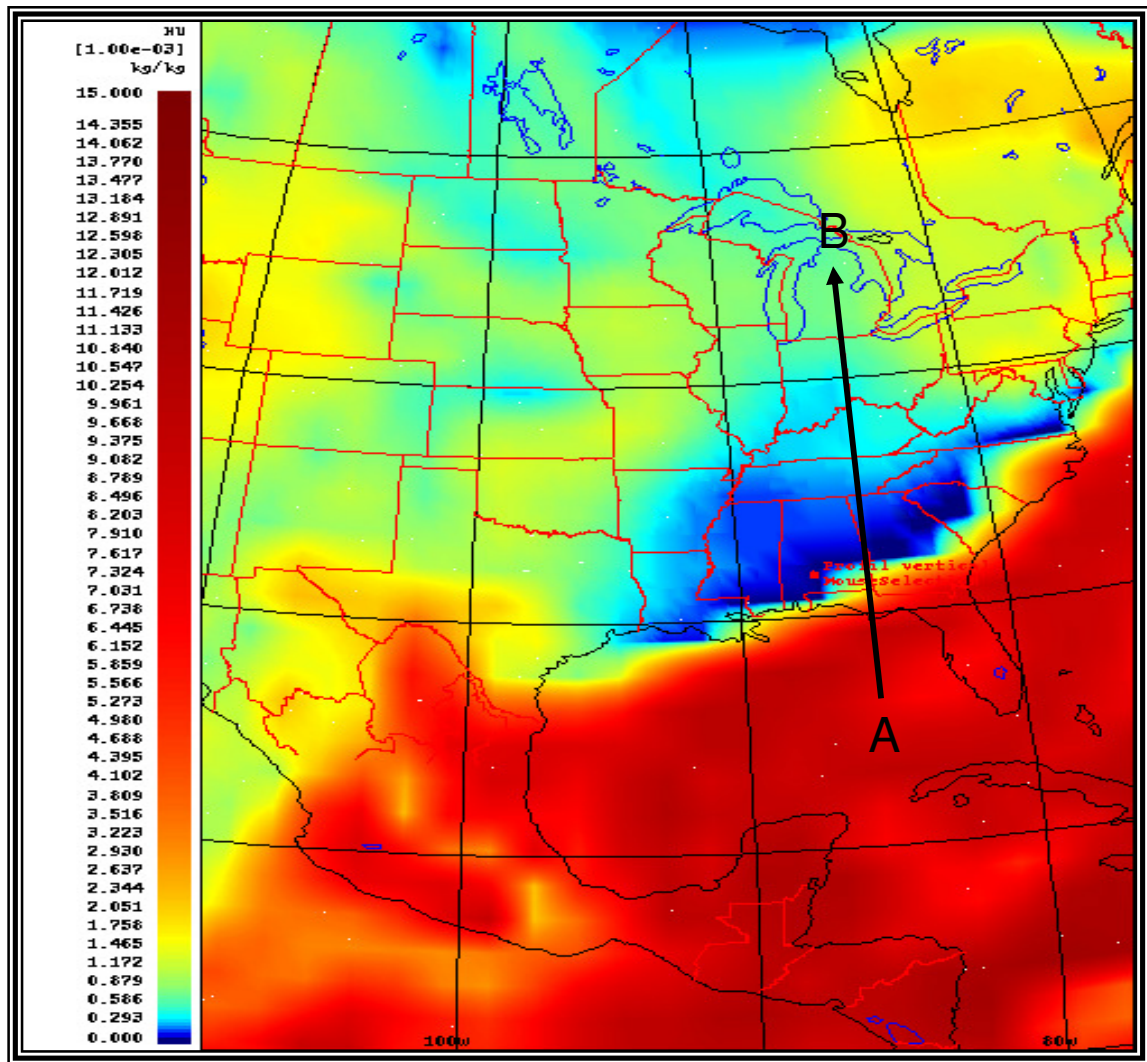
FIGURE 11

FIGURE 12

FIGURE 13

HYBRID

O₃ tongue

Tue Mar 14 2006, 18 UTC

A

B
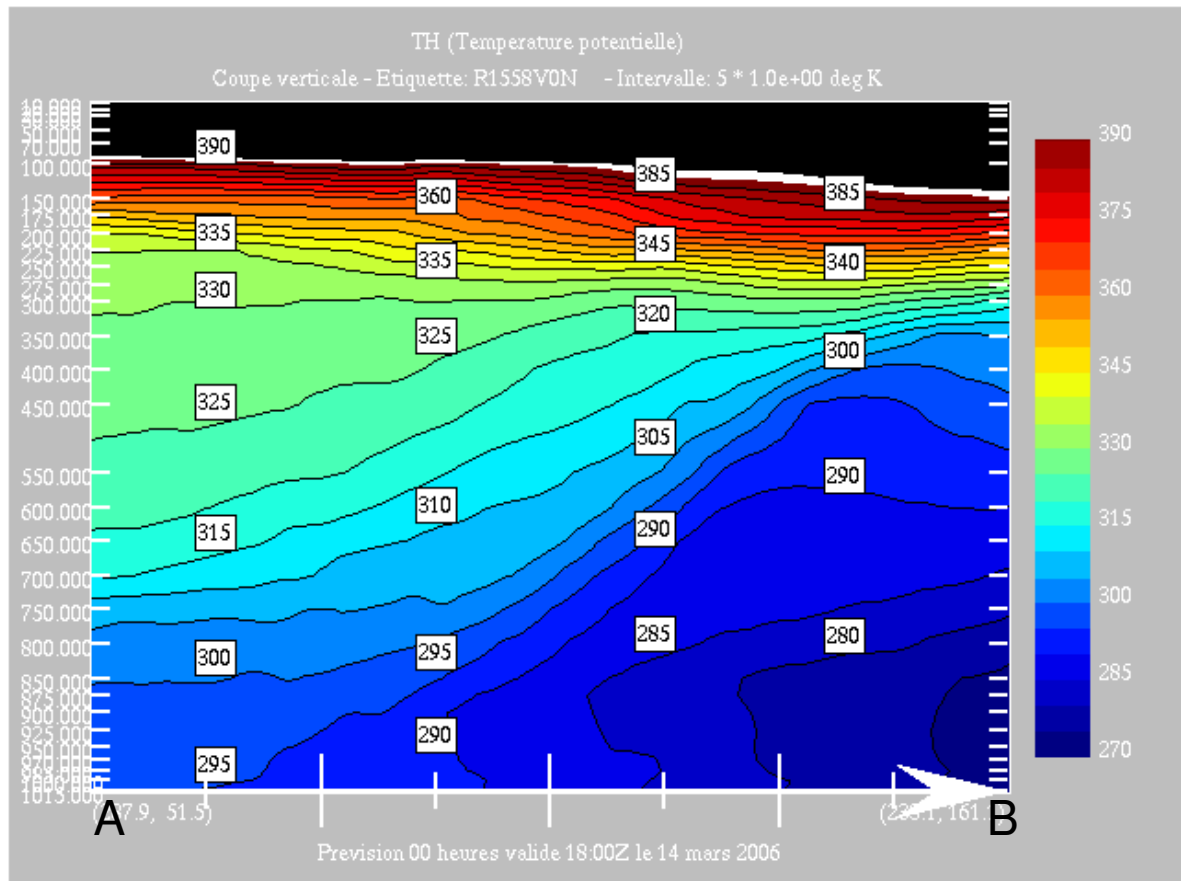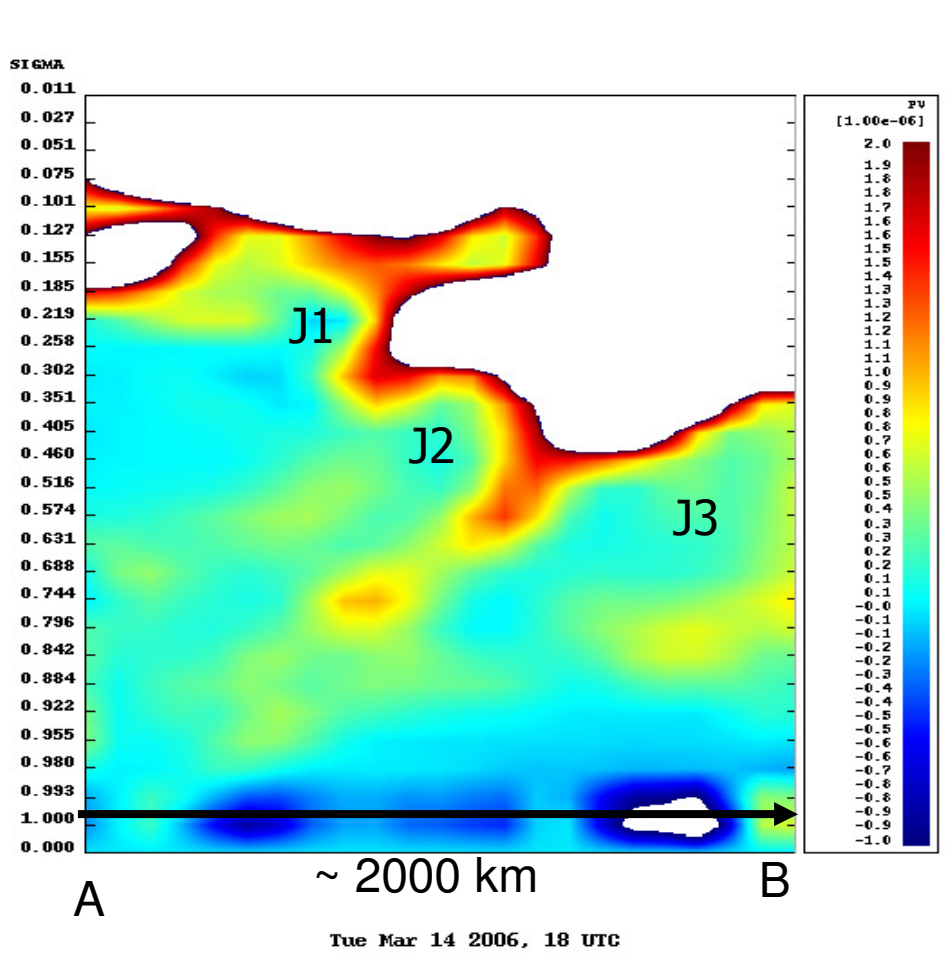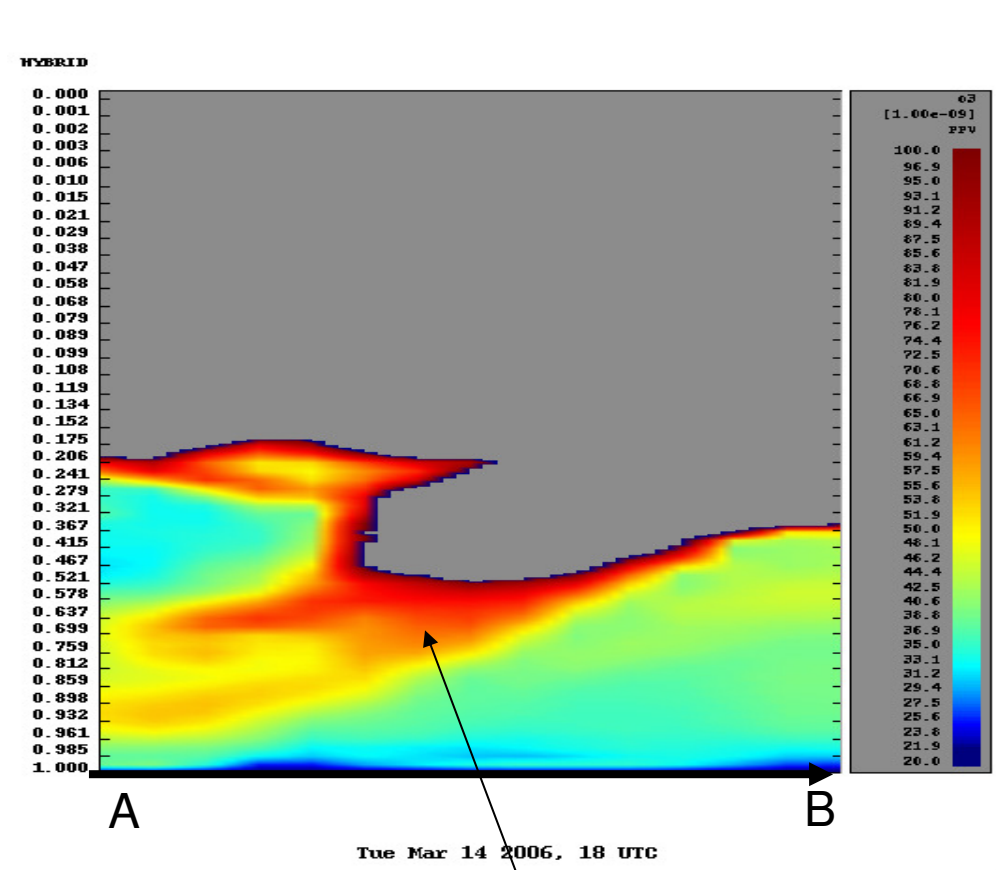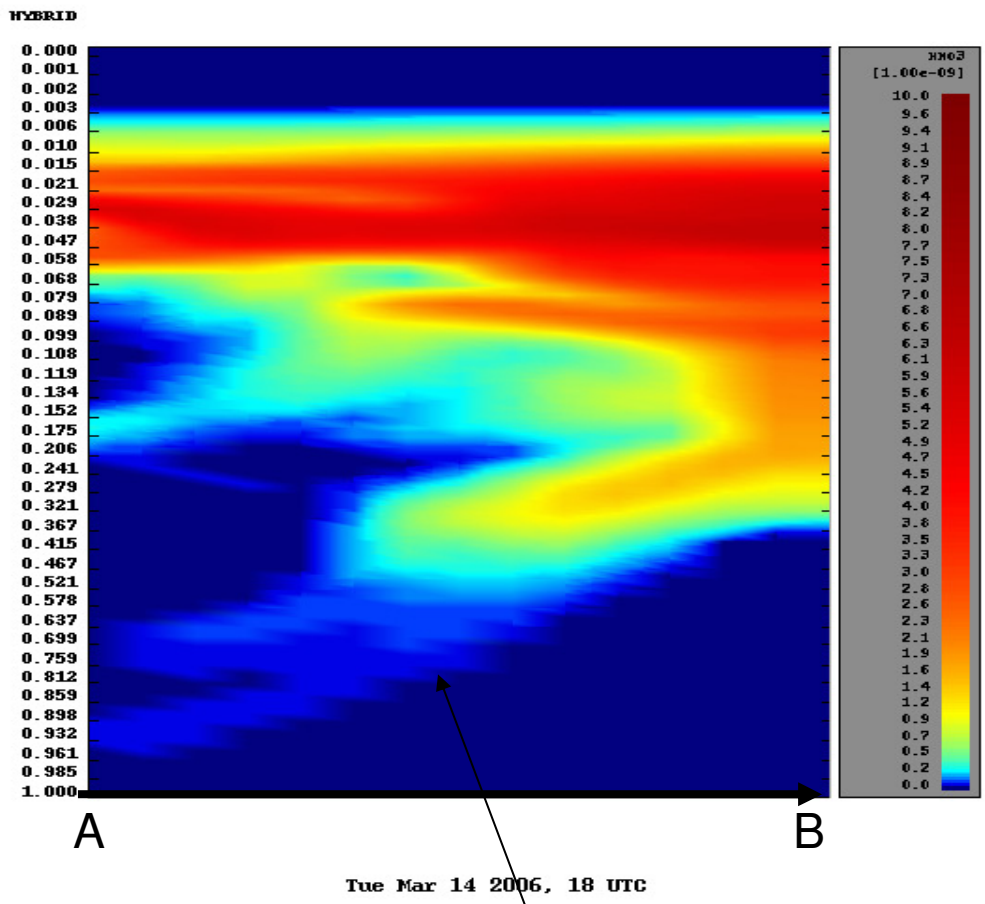
FIGURE 14A

HNO$_3$ tongue

FIGURE 14B
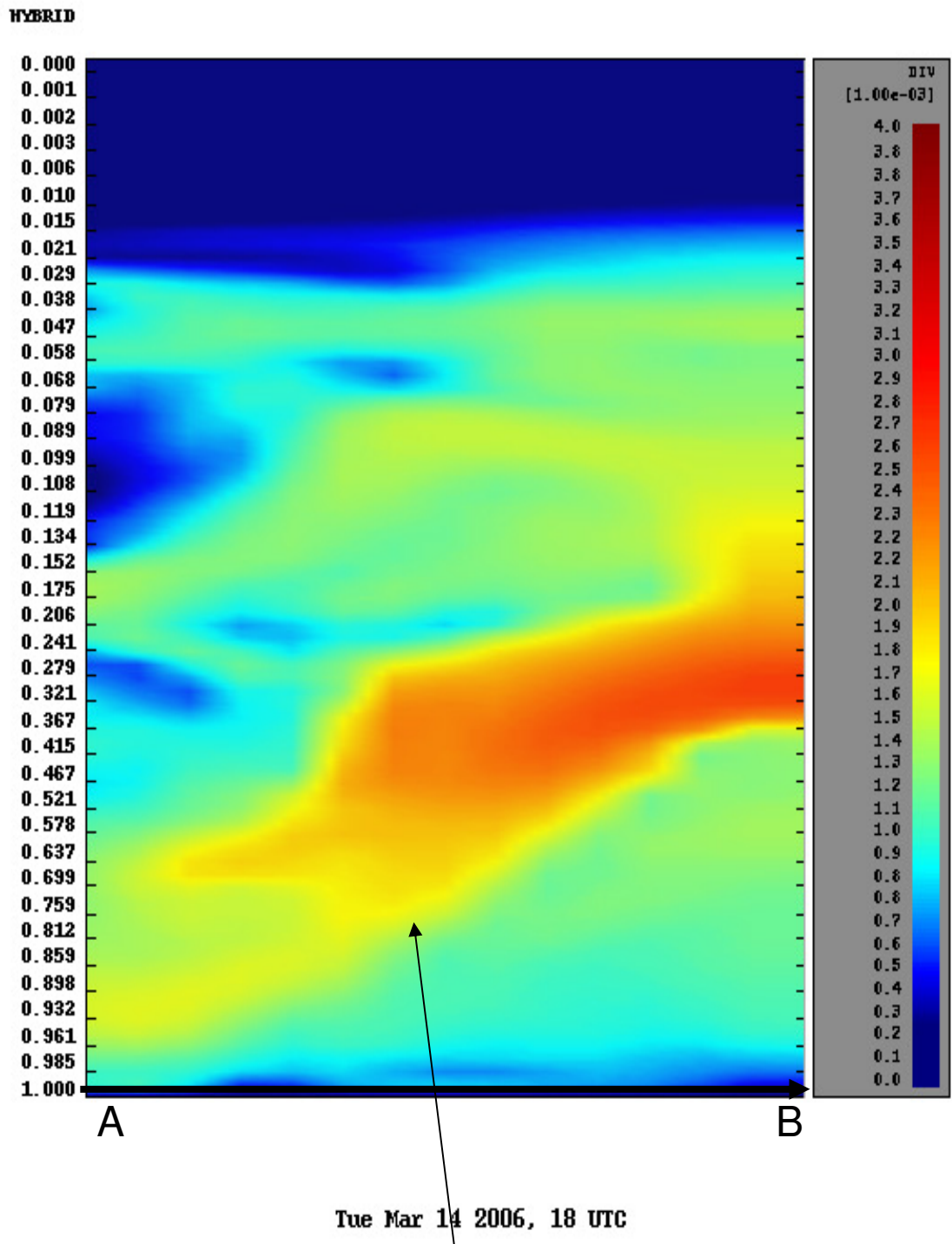
Signature of stratospheric intrusion

FIGURE 14C
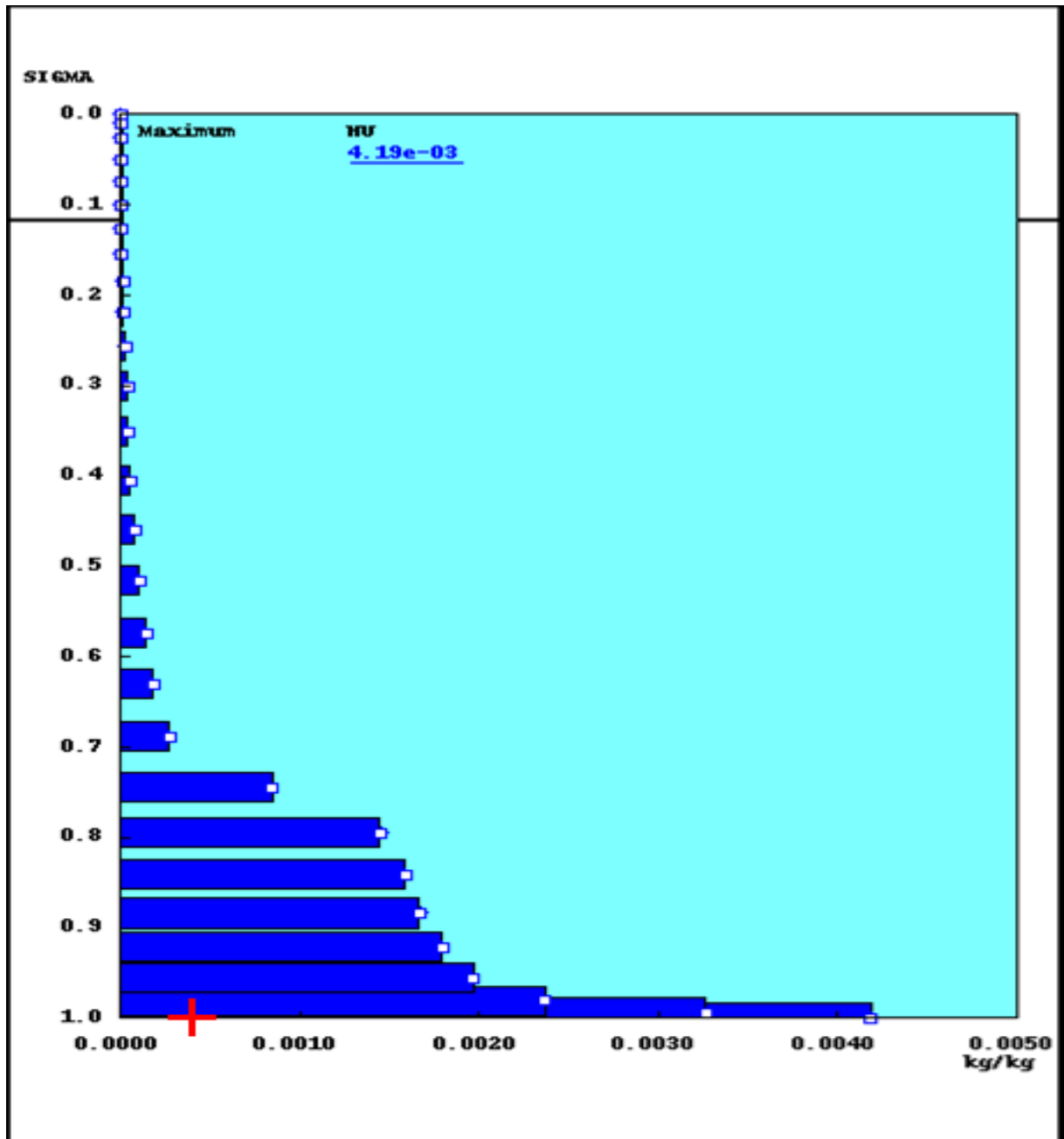
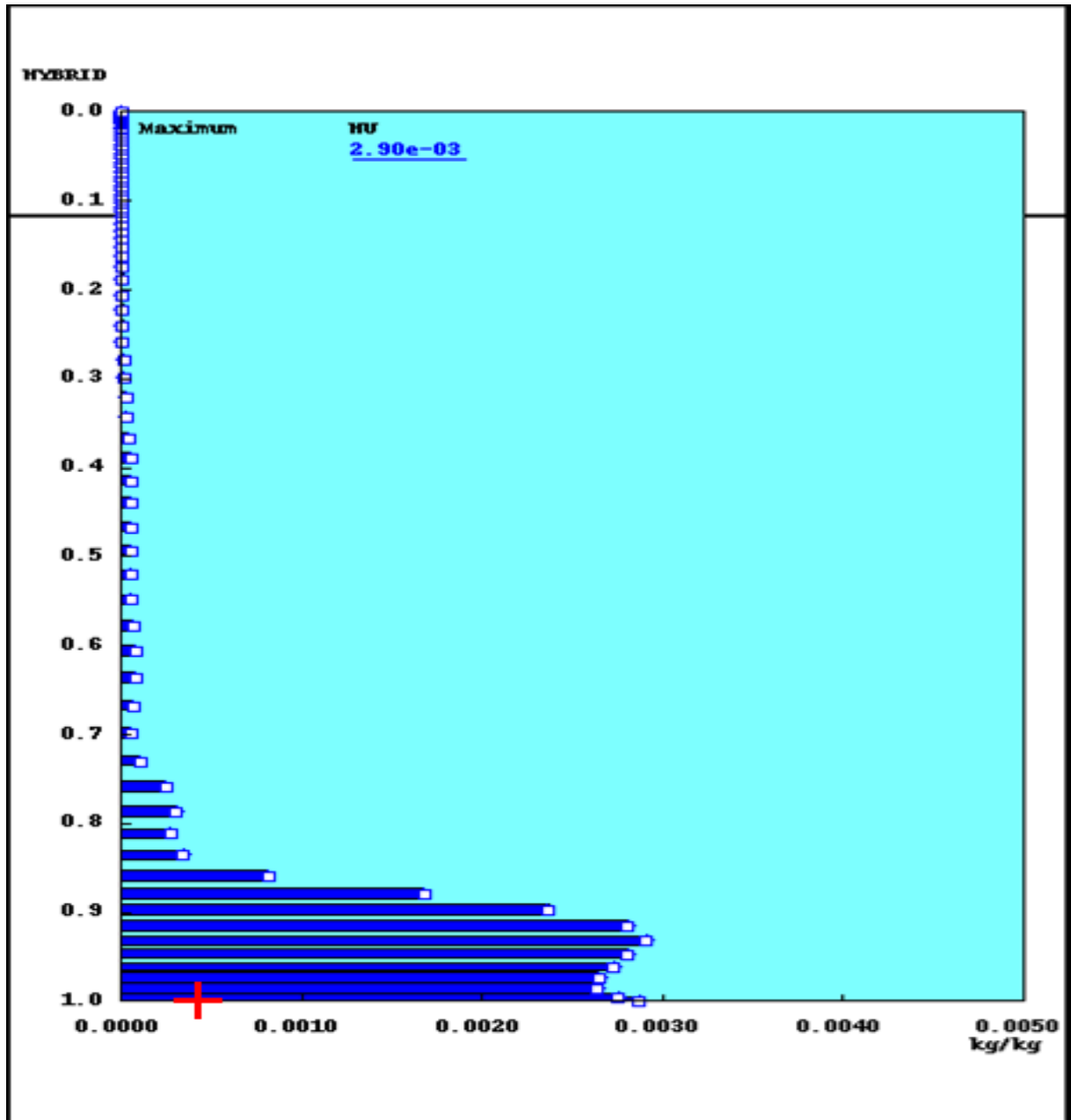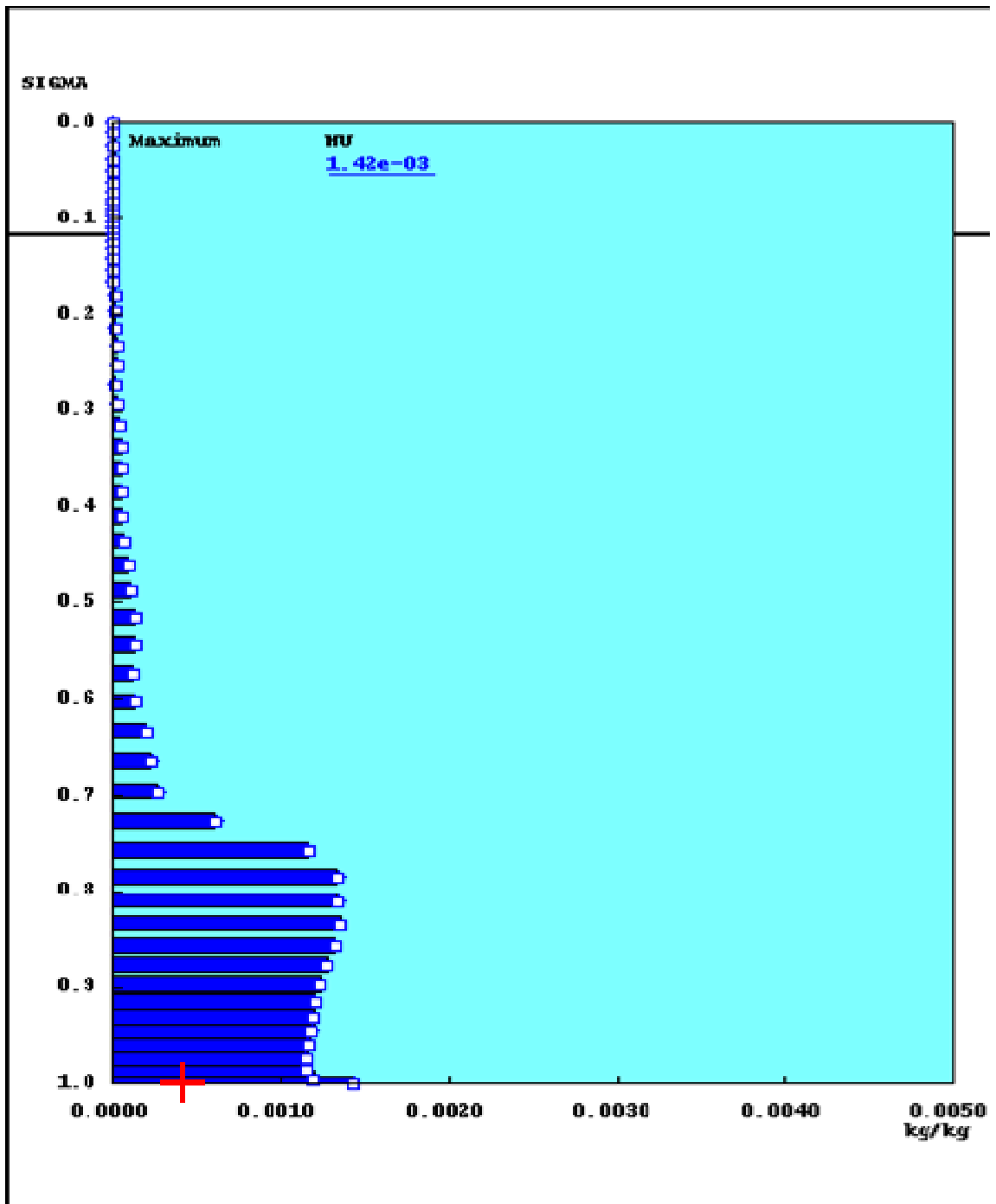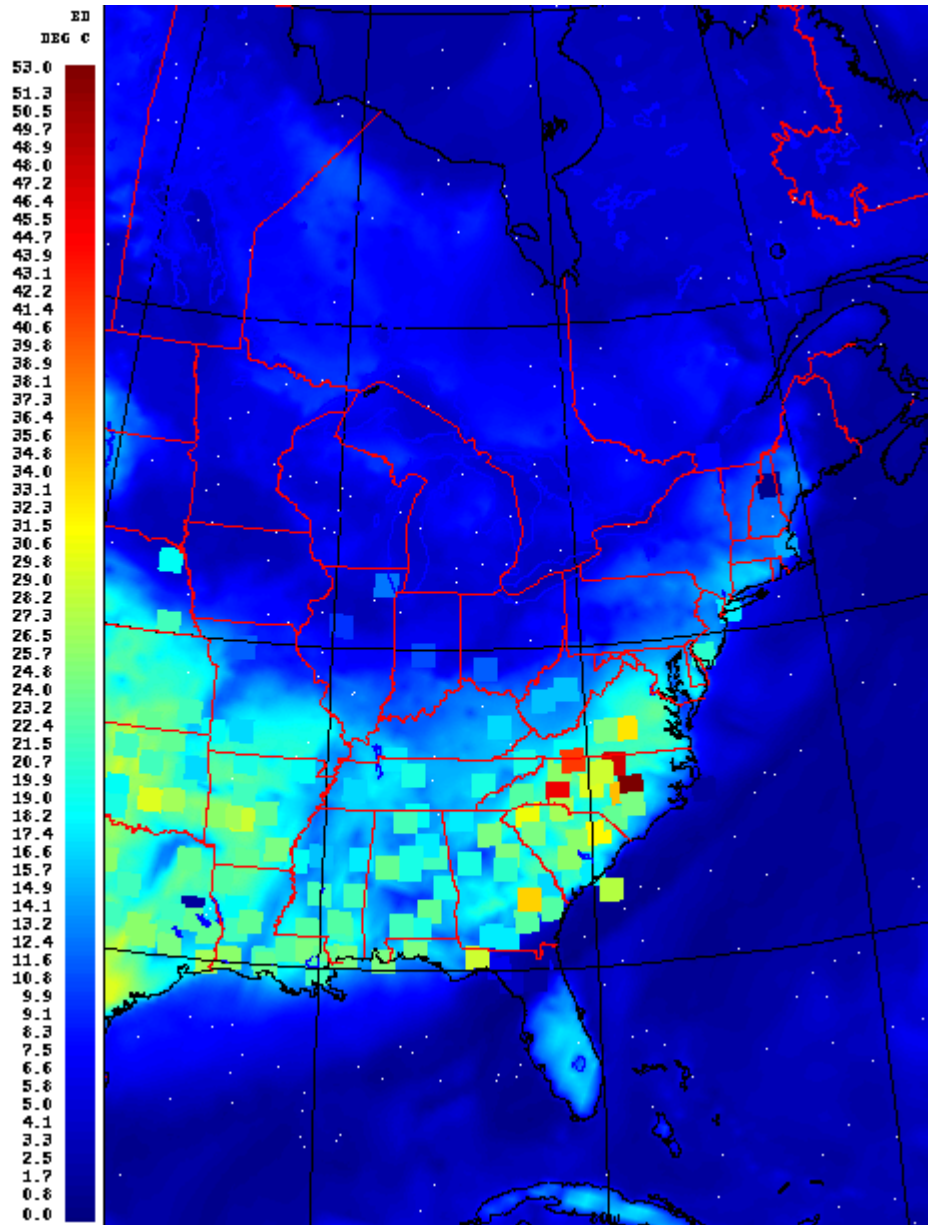**FIGURE 15A.**

FIGURE 15B.

FIGURE 15C.

FIGURE 16

FIGURE CAPTION

Figure 1. CMC surface analysis on March 14th 2006 at 18Z.

Figure 2. Windspeed (kts) at 250 hPa on March 14th 2006 at 18Z from GEM-Global model.

Figure 3. Geopotential height at 250 hPa on March 14th 2006 at 18Z. The dotted circles indicate the base of the trough in the height field and also the estimated position of the tropopause folding.

Figure 4. CMC wind analysis and height at 500 hPa on March 14th 2006 at 12Z.

Figure 5. Infrared GOES-12 satellite image on March 14th 2006 at 22:15Z.

Figure 6. Water vapour channel GOES-12 satellite image on March 14th 2006 at 18:15Z.

Figure 7. Surface ozone objective analysis on March 14th 2006 at 22 Z: a) CHRONOS output (top left panel), b) OA (top right), c) analysis increment (bottom left) and d) AIRNOW observations (bottom right).

Figure 8. Total ozone column (DU) as measured by OMI on March 14th 2006.

Figure 9. Geographical map of selected METAR stations.

Figure 10. Time series of surface relative humidity for selected METAR stations.

Figure 11. Water vapour mixing ratio at the top of the boundary layer on March 14th 2006 18Z (from GEM-Regional model).

Figure 12. North-South cross section A-B of the potential temperature along 85°W on March 14th 2006 18Z (from GEM-Regional model).

Figure 13. North-South cross section A-B of potential vorticity (white areas indicate values equal or greater than 2 PVU) along 85°W on March 14th 2006 18Z (from GEM-Regional model).

Figure 14. North-South cross section A-B along 85°W on March 14th 2006 18Z from GEM-MSC-BIRA for a) Ozone (ppv), b) HNO3 (ppv) and c) HNO_3/O_3.

Figure 15 A. Vertical profile of water vapour mass mixing ratio over KJNX (North Carolina) on March 15th 2006 at 00Z for a) GEM-Global, b) GEM-MSC-BIRA, c) GEM-Regional. The surface observation is depicted as a red cross.

Figure 16. Model values of surface dew point depression (^{o}C) (background color) as compared with observed values from METAR (colored squares) on March 14th 2006 at 21Z (from GEM-Regional).